MONTANA STATE UNIVERSITY

Optimization of the number of elements for thermal maps utilizing Radtherm/RT
by Allison Elizabeth Bristow

A thesis submitted in partial fulfillment of the requirements for the degree of Master of Science in Mechanical Engineering
Montana State University
© Copyright by Allison Elizabeth Bristow (2003)

Abstract:
In this thesis an analytical approach was used to optimize the number of elements required to produce accurate thermal maps utilizing RadTherm/RT. RadTherm/RT is a thermal model that uses all modes of heat transfer to predict road temperatures. The goal is to maximize the length of highway modeled and minimize the computation time. A methodology is implemented using a 4-part C/C++ algorithm to select particular elements to delete. The section of code that specifically determines the elements to delete is referred to as the view factor trim routine.

Initial steps are performed in order to obtain the information needed to determine the elements to delete. First, two files are necessary to create a new project in RadTherm/RT. Montana State University's Geographic Information and Analysis Center produced the ASCII files for elevation, road and vegetation maps using ARC/INFO GIS software. These files are loaded into RadTherm/RT to create a new project (.tdf). The project is executed to produce the view factor file (.vfs). Geometric view factors are used as the basis to eliminate elements. Radiation view factors are used in ThermoAnlaytics' software to determine the intensity of radiation of each element to every other element in the model and to the environment. This allows the terrain model to include full effects of solar shadowing, multiple reflections, and reradiation of geometric objects. The geometric view factors of each element are calculated using ThermoAnalytics Ray Trace Algorithm and the results are stored in the view factor file (.vfs).

Two text files are required as input into the view factor trim routine. The first file contains the view factor information. This file is obtained by applying an algorithm written by ThermoAnalytics. The routine converts the view factor file (.vfs), which is in HDF format, to a text file. A second file is obtained by applying a routine that retrieves each element and its attributes, which includes the element number, part number, UTM coordinates, and elevation.

The view factor trim routine uses the element attributes and view factor information text files to determine which elements to delete from the model. The routine was developed to have the capability of designating any part(s) as the elements of interest, which are the elements of primary interest for temperature. Furthermore, the values used for the criteria to determine which elements to delete can be modified. The first criterion is the distance from the elements of interest, where all elements that meet this criterion are kept. The next criterion determines the minimum view factor value to keep an element that directly exchanges radiation with an element of interest. Similarly, a minimum view factor criterion is set for elements that emit to or receive energy from elements that have a direct radiation exchange to the elements of interest. The result from the view factor trim routine is a text file that contains the elements to delete.

The final part of the code uses the text file that contains the elements to delete and creates a new project in RadTherm/RT. The primary difference in the new project is that it contains a new part composed of the elements to delete. This allows a user to view the elements, before deleting them.

OPTIMIZATION OF THE NUMBER OF ELEMENTS FOR THERMAL MAPS UTILIZING RADTHERM/RT

by

Allison Elizabeth Bristow

A thesis submitted in partial fulfillment
of the requirements for the degree

of

Master of Science

in

Mechanical Engineering

MONTANA STATE UNIVERSITY – BOZEMAN
Bozeman, Montana

September 2003

© COPYRIGHT

by

Allison Elizabeth Bristow

2003

All Rights Reserved

N378
B773

APPROVAL

of a thesis submitted by

Allison Elizabeth Bristow

This thesis has been read by each member of the thesis committee and has been found to be satisfactory regarding content, English usage, format, citations, bibliographic style, and consistency, and is ready for submission to the College of Graduate Studies.

Dr. Edward E. Adams — (Signature) — 3-SEPT-2003 — Date

Approved for the Department of Mechanical and Industrial Engineering

Dr. Vic A. Cundy — (Signature) — 9/3/03 — Date

Approved for the College of Graduate Studies

Dr. Bruce R. McLeod — (Signature) — 9-8-03 — Date

STATEMENT OF PERMISSION TO USE

In presenting this thesis in partial fulfillment of the requirements for a master's degree at Montana State University – Bozeman, I agree that the library shall make it available to borrowers under rules of the Library.

If I have indicated my intention to copyright this thesis by including a copyright notice page, copying is allowable only for scholarly purposes, consistent with "fair use" as prescribed in the U.S. Copyright Law. Requests for permission for extended quotation from or reproduction of this thesis (paper) in whole or in parts may be granted only by the copyright holder.

Signature

Date 9/2/03

TABLE OF CONTENTS

1. CHAPTER 1 INTRODUCTION 1

2. CHAPTER 2 BACKGROUND 6

HEAT TRANSFER 6
Conduction 6
Convection 7
Radiation: Processes and Properties 7
Shortwave Radiation 9
Longwave Radiation 9
Radiation Exchange Between Surfaces 10
Surface Absorption, Reflection, and Transmission 10
Surface Emission 12
View Factor 12
RADTHERM/RT HEAT TRANSFER 23
Interior Layer Energy Balance 28
Surface Energy Balance 29
Energy Storage 30
Air Convection 30
Precipitation Convection 30
Ground Layer Conduction 31
Solar Load 31
Expanding Governing Equation 34
Net-radiation Method – Enclosure Theory 35
NUMERICAL METHOD OF SOLUTION 41
Transient Formulation 42
Computation of Temperature Distribution 44

3. CHAPTER 3 METHODOLOGY 46

RAY-TRACING ALGORITHM 46
View Factor Rays 49
View Factor Subdivisions 50
Apparent Area Resolution 50
Hand Calculation for View Factor 51
THE PROCESS TO DELETE ELEMENTS 52
Initial Setup 54
Step 1a - Digital Elevation Map Files (.asc) 54
Step 1b - Terrain File (.asc) 55
Step 2 - Trimming the Original Map 58

TABLE OF CONTENTS - CONTINUED

Step 3 - RadTherm/RT Project Files (.tdf) 60
Step 4 - Element Attribute File 63
Step 5 - View Factor File (.vfs) 65
Step 6 – Code to Delete Elements 68
Step 6a – Separate Elements. 69
Step 6b – Apply Distance Criteria 70
Step 6c – View Factors to Elements of Interest. 71
Step 6d – View Factors to Elements with View Factors to Elements of Interest. 73
Step 6e – Output File 75
Step 7 – Create a new part 76
Creating a RadTherm Project 76

4. CHAPTER 4 FINDINGS/RESULTS 80

RADIATION EXCHANGE – SIMPLE MODEL 80
Shadowing Effects 81
Shortwave Radiation Exchange 84
180° Flat Model 85
135° Model 87
90° Model 92
Longwave Radiation Exchange 98
MODEL OF BOZEMAN PASS 104
No View Factor or Distance Criteria 111
No View Factor and Distance Criteria Set 113
View Factor and Distance Criteria Set 115
Evaluate View Factor Criterion 115
Results 118
MODEL OF ROCKY CANYON 120
Coordinates for Rocky Canyon Model 120
Assign RadTherm/RT Part ID. 123
Location for Temperature Comparison 127
Summer Test Case – July 2nd, 2003 129
Weather File - Summer 129
Temperature Comparison – Mile Marker 315 131
Temperature Comparison – Mile Marker 315½ 132
Temperature Comparison – Mile Marker 316 132
Temperature Comparison – Mile Marker 316½ 133
Temperature Comparison – Mile Marker 317 133
Temperature Comparison – Mile Marker 317½ 135

TABLE OF CONTENTS - CONTINUED

Temperature Comparison – Mile Marker 318 135
Winter Test Case – February 2nd, 2003 136
Weather File - Winter 136
Temperature Comparison – Mile Marker 315 137
Temperature Comparison – Mile Marker 315½ 137
Temperature Comparison – Mile Marker 316 140
Temperature Comparison – Mile Marker 316½ 140
Temperature Comparison – Mile Marker 317 141
Temperature Comparison – Mile Marker 317½ 142
Temperature Comparison – Mile Marker 318 143

5. CHAPTER 5 SUMMARY/CONCLUSIONS 144

6. REFERENCES CITED 150

7. APPENDICES 152

APPENDIX A: C/C++ CODE – RETRIEVE ELEMENT ATTRIBUTES 153
APPENDIX B: C/C++ CODE – VIEW FACTOR TRIM ROUTINE 160
APPENDIX C: C/C++ CODE – UPDATE RADTHERM PROJECT FILE 179

LIST OF TABLES

Table Page

1. View factor ray setting in RadTherm/RT. 50
2. View factor ray setting in RadTherm/RT. 52
3. Land cover classification system used by Montana Gap Analysis Project.... 56
4. Summary of the iterations for trimming a map of Bozeman Pass to a size that produces the view factor file (.vfs). 59
5. Solar Azimuth and Zenith angles at two-hour increments on July 22, 1993.....83
6. (a) View factor values for Figure 48a. Receiver #17 is the sky node. (b) View factor values for Figure 48b. Receiver #26 is the sky node. 87
7. The absorptivity values for the sloped terrain for each case.... 88
8. View factors for Element 10 labeled on Figure 50b with $\theta = 135°$. (a) Shows the receiving elements that element 10 emits to. Note that receiver number 26 is the sky node. (b) The elements that emit to element 10. 89
9. View factors for Element 10 labeled for a rock wall at 135°, and for a rock wall at 90°. 93
10. The percentage of the view factor values for element 40 in each model in Figure 60. 100
11. Results for the model of Bozeman Pass with the distance criterion and view factor criteria set to zero. For this case, 82,075 elements were deleted.....112
12. Results for the model of Bozeman Pass with the distance criterion set to 250-meters and the view factor criteria set to zero. For this case, 81,448 elements are deleted. 113
13. The emissivity values for the terrain types in RadTherm/RT.... 116

LIST OF TABLES - CONTINUED

Table Page

14. Results for the model of Bozeman Pass with the distance criterion set to 250-meters and the view factor criteria set to 0.0005. For this case, 288,308 elements are deleted. 118

15. Results for Rocky Canyon using the view factor trim routine with the distance criteria set to 0 and the view factor criteria set to 0.0005. 123

16. Land cover classifications mapped to RadTherm/RT part ID's. 125

17. Each RadTherm/RT part and the associated properties. 127

18. The temperatures are compared at each ½ mile between mile marker 315 and 318. The UTM coordinates and element numbers at listed for each location. 128

LIST OF FIGURES

Figure Page

1. Electromagnetic Spectrum (After Incropera and DeWitt, 1996, Figure 12.3).....8

2. Absorbed, reflected, and transmitted shortwave radiation with a semitransparent medium. 11

3. Radiation emitted by a surface. (a) Spectral distribution. (b) Directional distribution. (After Incropera and DeWitt, 1996, Figure 12.4).....13

4. Radiation emitted from a point in differential area dA_1 into a solid angle $d\omega$ subtended by differential area dA_n. (After Incropera and DeWitt, 1996, Figure 12.5).....14

5. (a) Definition of a plane angle. (b) Definition of a solid angle. (After Incropera and DeWitt, 1996, Figure 12.6).....15

6. In the spherical coordinate system, a solid angle subtended by dA_n from a point on dA_1. (After Incropera and DeWitt, 1996, Figure 12.7).....16

7. Two surface normals of the differential areas dA_i and dA_j. θ_i and θ_j are the angles to the line connecting the two bodies. 17

8. The projection of dA_i and dA_j normal to the direction of radiation. 17

9. The differential solid angle subtended by dA_j from a point on dA_i. 18

10. A diffuse reflector. 20

11. Surface radiosity. 21

12. A mesh created for RadTherm/RT for a region of interest. 24

13. A single soil element and the associated layers. 25

14. Heat transfer modes for each node.....26

15. Angle of incidence. 33

LIST OF FIGURES - CONTINUED

Figure Page

16. Energy quantities incident upon and leaving a typical surface of an enclosure 37

17. The position of the sun is specified in terms of the zenith and azimuth angles, θ and ϕ, respectively.....48

18. (a) A single ray cast from an element for ThermoAnalytics Ray Trace Algorithm. (b) Multiple rays cast from an element for ThermoAnalytics Ray Trace Algorithm. (Figures from ThermoAnalytics, Inc. website).....49

19. (a) A simple model used for the hand calculation of the view factor. The model consists of two finite rectangles of the same length, having one common edge at an angle of 90° to each other. (b) The equation used to calculate the view factor from *1* to *2*. (After Siegel and Howell, Figure 16 in the Appendix) 51

20. Example of ASCII input file for elevation data created from USGS 30 meter grid.....55

21. Example of the ASCII input file for the terrain and road information. This file has been converted from the land classification to RadTherm/RT Part ID's. Note that 1 represents a part ID such as the road.....57

22. Command line to execute the gis_manip PERL script. 59

23. (a) Set each part to type terrain. (b) Specify a weather file. (c) Set the same start and end solution times.....61

24. Flow chart of Steps 1 through 3. Step 1 is generating the ASCII files. Step 2 determines the UTM coordinates for a map with less than 330,000 elements. Step 3 creates a new project in RadTherm/RT. 62

25. Example of a RadTherm/RT project composed of 2 parts. 63

26. Step 4 of the procedure. A C/C++ code is used to create a text file with the element attributes: Element ID, Part ID, UTM coordinates, and elevation.....64

27. Example of the text file that contains the element attributes. This is the output file from Step 4. 65

LIST OF FIGURES - CONTINUED

Figure Page

28. Flow chart for Step 5. This step converts the view factor file to an ASCII text file..... 66

29. The command line to execute the vf2asc utility 66

30. This is the output file from Step 5. Example of the view factor file produced from the vf2asc executable. 67

31. Flow chart for an overview of Step 6. The Element Attribute text file and View factor text file are used as input into Step 6. The output from Step 6 is a text file containing the elements to delete. 68

32. Flow chart for Step 6a. This step separates all the surface elements for the terrain map into two categories. The first category is the elements of interest with a rank of 1 and the second category is the surrounding elements with a rank of 2. 69

33. A simple demonstration terrain model to describe the ranking after Step 6a. 70

34. Simple demonstration terrain model to describe the ranking after Step 6b. 71

35. Illustrates the three options for Step 6c. The emitter is an element of interest, or the receiver is an element of interest, or neither the emitter nor receiver is an element of interest. 72

36. Simple demonstration terrain model to describe the ranking after Step 6c. 73

37. Simple demonstration terrain model to describe the ranking after Step 6d. 74

38. Summary of the ranks applied to the elements in Steps 6a, 6b, 6c, and 6d. 75

39. An example of the output text file from Step 6e. The first row of the file contains the number of elements to delete. The subsequent rows are the element numbers to delete (R = 1). 76

40. Summary of steps 6b through 6e. 77

LIST OF FIGURES - CONTINUED

Figure Page

41. Flow chart for Step 7. The elements to delete, which are contained in the text file, are assigned to a new Part ID. 78

42. Example of the new update.tdf project created for RadTherm/RT. A new part has been created (Part 18) labeled "Elements to Delete". 79

43. Example of the update.tdf project after Part 18, which contains the elements to delete, has been removed 79

44. Simple model to demonstrate importance of shading. A represents the interstate and B represents a wall of rock. 81

45. A simple model that represents a flat highway. 82

46. A temperature plot for element 6 of the interstate without a rock wall versus element 6 of the interstate with a rock wall. The plot is from 12:00 AM on July 22, 1993 to 12:00 PM on July 23, 1993. 83

47. The side view of a model with a sloped rock wall with a varying angle θ. 84

48. (a) Simple model of the interstate with fifteen surface elements. (b) Simple model of the interstate with an adjoining terrain part composed of nine surface elements (16-24) and modeled as rock. 85

49. Plot of the 24-hour temperature output for Element 10 for both models described in Figure 48b. 86

50. (a) Side view of the model with the sloped wall at an angle of 135°. (b) A model composed of two parts. Part A is the interstate with fifteen elements. Part B is the sloped wall at 135° from the interstate. 88

51. The temperature plot for Element number 10 for two cases. A rock slope with: 1) an absorptivity (α) of 0.05 and 2) $\alpha = 0.90$ 91

52. The temperature plot for Element number 20 for both cases. For the first case, the rock slope has an absorptivity (α) of 0.05 and in the second case, $\alpha = 0.90$. Element 20 is the center element on the sloped terrain. 92

LIST OF FIGURES - CONTINUED

Figure Page

53. (a) Side view of the simple model consisting of two parts, the interstate and a rock wall at and angle of 90°. (b) A simple RadTherm/RT model consisting of two parts, the interstate and a rock wall at 90°. Fifteen elements are assigned to the interstate and nine elements are assigned to the rock wall at 90°. 92

54. The temperature plot for Element 10 for both cases. For the first case, the rock slope has an absorptivity of 0.05 and in the second case has an absorptivity of 0.90. 94

55. The temperature plot for 90 degree wall, Element 20 for two cases. With a rock slope that has 1) an aborptivity (α) of 0.05 and 2) $\alpha = 0.90$. 95

56. The highway temperature of Element 10 for the model with a sloped terrain at 135° and 90° with an absorptivity value of 0.90. 96

57. The temperature plot of Element 10 for the model with terrain sloped at 135° and 90° with an absorptivity value of 0.05. 97

58. Side view of the models used to compare the longwave radiation effects. (a) Simple model without a left rock wall. (b) Simple model with a rock wall on the left side. 98

59. The model used to compare the longwave radiation effects with the pertinent elements labeled. 100

60. The temperature plot of interstate element 40 for both models. Note that the solar radiation is set to zero at 9:50 AM. 101

61. The temperature plot of Element 40 where the left rock wall increases in 10-meter segments 102

62. A plot of the temperature of interstate Element 40 to Element 112 on the left rock wall 103

63. A plot of the temperature of interstate Element 40 (with no left wall) to the sky temperature for the model. 104

LIST OF FIGURES - CONTINUED

Figure Page

64. The UTM coordinates used to create the model for Bozeman Pass. 104

65. RadTherm/RT model for Bozeman Pass consisting of 327,610 surface elements and 17 parts. 105

66. The Part ID that contains the elements of interest must be specified. The two lines of code that must be set for Step 6 are labeled A and B. 107

67. A simple model to illustrate the distance criterion set at 100 meters. 108

68. The distance criterion in Step 6b is assigned in the code, which is labeled as C. In this case, the distance criterion is 250 meters. 109

69. The view factor criteria must be set for lines D and E. In this case, the view factor criteria are 0.0005. 109

70. This is the identical model as in Figure 65, but contains an additional part. This part (Part 18) contains the elements to delete. 110

71. A magnified picture of the interstate through Bozeman Pass. The empty spaces are a result of the deleted elements. 112

72. The resulting model of Bozeman Pass with the distance criterion set to 250 meters and the view factor criteria set to zero. Only 82,000 surface elements have been deleted and 245,000 surface elements remain in the model. 114

73. Plot of Equation (81), which is the energy lost or gained from surface element k to j. The x-axis is the radiation from surface element j and varies from 0 to 50,000 Watts. The graph plots the radiation term of surface k for four different temperature values of j. 117

74. The resulting model of Bozeman Pass with the distance criterion set to 250 meters and the view factor criteria set to 0.0005. 288,308 surface elements have been deleted and 39,302 surface elements remain in the model. 119

LIST OF FIGURES - CONTINUED

Figure Page

75. The region selected for the model of Rocky Canyon. The interstate spans from mile marker 314½ to mile marker 318. 121

76. A 3-dimensional map of Interstate 90 through Rocky Canyon from mile marker 314 heading east. 121

77. RadTherm/RT model for Rocky Canyon consisting of 33,096 surface elements. 122

78. RadTherm/RT model for Rocky Canyon after the view factor trim routine is applied. The distance criterion was set at zero and the view factor criteria were set at 0.0005. This model consists of 5,777 surface elements. 124

79. An example of the RadTherm/RT GUI for a foliage terrain part. 126

80. Meteorological Plots from 12:00 am on July 2nd, 2003 for (a) air temperature vs. time (b) solar radiation vs. time (c) cloud cover verse time of day. 130

81. (a) Temperature comparison for element 17775 (original map) verse element 4545 (map with deleted elements) for July 2nd, 2003. (b) Difference in Temperature between the original map and the trimmed map. 131

82. (a) Temperature comparison for element 19009 (original map) verse element 4964 (map with deleted elements) for July 2nd, 2003. (b) Difference in Temperature between the original map and the trimmed map. 132

83. (a) Temperature comparison for element 14329 (original map) verse element 3310 (map with deleted elements) for July 2nd, 2003. (b) Difference in Temperature between the original map and the trimmed map. 133

84. (a) Temperature comparison for element 10832 (original map) verse element 1903 (map with deleted elements) for July 2nd, 2003. (b) Difference in Temperature between the original map and the trimmed map. 134

85. (a) Temperature comparison for element 10494 (original map) verse element 1813 (map with deleted elements) for July 2nd, 2003. (b) Difference in Temperature between the original map and the trimmed map. 134

LIST OF FIGURES - CONTINUED

Figure Page

86. (a) Temperature comparison for element 7388 (original map) verse element 810 (map with deleted elements) for July 2nd, 2003. (b) Difference in Temperature between the original map and the trimmed map. 135

87. (a) Temperature comparison for element 5470 (original map) verse element 379 (map with deleted elements) for July 2nd, 2003. (b) Difference in Temperature between the original map and the trimmed map. 136

88. Meteorological Plots from 12:00 am on February 2nd, 2003 for (a) air temperature vs. time (b) solar radiation vs. time (c) cloud cover verse time of day 138

89. (a) Temperature comparison for element 5470 (original map) verse element 379 (map with deleted elements) for February 2nd, 2003. (b) Difference in Temperature between the original map and the trimmed map. 139

90. (a) Temperature comparison between element 19009 (original map) verse element 4964 (map with deleted element) for February 2nd, 2003. (b) Difference in Temperature between the original map and the trimmed map.....139

91. (a) Temperature comparison between element 14329 (original map) verse element 3310 (map with deleted element) for February 2nd, 2003. (b) Difference in Temperature between the original map and the trimmed map.....140

92. (a) Temperature comparison between element 10832 (original map) verse element 1903 (map with deleted element) for February 2nd, 2003. (b) Difference in Temperature between the original map and the trimmed map.....141

93. (a) Temperature comparison between element 10494 (original map) verse element 1813 (map with deleted element) for February 2nd, 2003. (b) Difference in Temperature between the original map and the trimmed map.....141

LIST OF FIGURES - CONTINUED

Figure Page

94. (a) Temperature comparison between element 7388 (original map) verse element 810 (map with deleted element) for February 2nd, 2003. (b) Difference in Temperature between the original map and the trimmed map.....142

95. (a) Temperature comparison between element 5470 (original map) verse element 379 (map with deleted element) for February 2nd, 2003. (b) Difference in Temperature between the original map and the trimmed map.....143

NOMENCLATURE

A	Area (m^2)
C_{ak}	Air to ground convection conductor
C_{Ho}	Bare soil heat transfer coefficient
C_{kk}	Ground layer conduction
C_p	Specific heat at constant pressure (J/kg-K)
C_{Rain}	Rain convection conductor
CAP_{k_i}	Heat capacitance (J/ m^2-K)
d_i	Thickness of ground layers (m)
E	Emissive Power (W/m^2)
E_b	Emissive Power of Blackbody (W/m^2)
F_{i-j}	View Factor
G	Irradiation (W/m^2)
h_{fg}	Latent Heat of vaporization (J/kg)
$I_{\lambda,e}$	Emitted spectral intensity (W/m^2- K)
I_i	Intensity of radiation leaving surface i (W/m^2- K)
J_i	Radiosity (W/m^2)
k	Von Karmon constant
k	Thermal conductivity (W/m-K)
m	Mass (kg)

NOMENCLATURE - CONTINUED

n_i	Surface normal
n_j	Surface normal
N	Number of surfaces (or elements) in an enclosure
q	Heat transfer rate (W)
Q	Heat flux (W/m^2)
r	Distance between centers of differential areas (m).
t	Time (s)
T_a	Air temperature (K)
T_k	Temperature at the surface (K)
T_R	Rain temperature (K)
T_s	Absolute Temperature (K)
u	Specific internal energy (kJ/kg)
U	Total internal energy (kJ)
v	Average rain velocity (mm/hr)
v_a	Average Wind Velocity (m/s)
w	Soil moisture
W	rate at which work is performed (W)
ω_g	Volume fraction of surface soil moisture
w_k	Volume fraction of surface soil moisture
α	Absorptivity

NOMENCLATURE – CONTINUED

ε	Emissivity
λ	Wavelength (m)
ϕ	Azimuth angle (rad)
ρ	Reflectivity (Albedo)
ρ_a	Density of air (kg/m^3)
τ	Transmissivity
θ	Zenith angle (rad)
σ	Stefan-Boltzmann Constant
ω	Solid angle (sr)

CHAPTER 1

INTRODUCTION

The Western Transportation Institute (WTI) is collaborating with the Montana Department of Transportation (MDT), Meridian Environmental Technology Incorporated, The Montana Department of Federal Highways Administration, Montana State University Civil Engineering, and ThermoAnalytics Incorporated (TAI) on a project known as the Greater Yellowstone Regional Traveler and Weather Information System (GYRTWIS). Part of this project is to develop and integrate a pavement temperature thermal model to provide a more detailed temperature forecast for two mountain passes: Lookout Pass on the Montana-Idaho border and Bozeman Pass [Ballard, 2001]. The goal is to accurately provide current and forecast weather and road condition information to highway operators and users. The prediction of pavement temperatures is currently being provided to help decision makers improve winter road maintenance operations. It could also be used in the future to provide forecasts of icy conditions for travelers.

The idea for modeling sections of highway is based on the adaptation of computational models used by the U.S military for the prediction of vehicle infrared images. Two programs were developed as tools to model the surface temperatures of vehicles for use in infrared imagery. The origin of the one dimensional, first principles heat transfer software for which the pavement model is derived is the Thermal Contrast Model (TCM), initially developed for the U.S. Air Force and PRISM (Physically Reasonable Infrared Signature Mode), which was produced at Michigan Technological

University's Keweenaw Research Center in conjunction with the U.S. Army Tank-Automotive Command (TACOM) [Adams, 1999]. Basically, the infrared signature of a vehicle exposed to a set of meteorological conditions indicates the surface temperature of the vehicle. The three-dimensional modeled vehicles were composed of a collection of flat plates termed "facets". The terrain in the model was considered as background and originally represented as an isothermal, flat plate. The facet concept used for vehicles was extended and used to represent the terrain presently used in the thermal modeling software [Adams and McDowell, 1991].

The current modeling tool used to predict these surface temperatures is a Radiation based Thermal Model for Road Temperature (RadTherm/RT). RadTherm/RT is a thermal modeling tool intended for comprehensive heat management design and analysis. ThermoAnalytics developed the software in conjunction with Montana State University to predict and graphically display road and surrounding terrain temperatures. The software provides a tool to analyze and model terrain temperature utilizing 3-D radiation, convection, and 1-D conduction. The input into the software includes a digital 3D-faceted terrain representation, meteorological data, and time/location information.

Developments in Geographic Information Systems (GIS), and the availability of Digital Elevation Maps (DEM) make it possible to produce files for elevation, road, and vegetation maps. The vegetation in this context includes grass, forests, water, rock, soil, etc. The elevation data was compiled from a United States Geological Survey (USGS) DEM's at a 30-meter resolution. The weather file includes standard meteorological parameters such as air temperature, wind velocity, precipitation, relative humidity, and

radiation data. From USGS DEM's, the mesh of the model was created in 30-meter square sections. Once the files were loaded into RadTherm/RT the sections were further divided into triangular elements. The output from RadTherm/RT is the temperature map for each node in the system.

The first step in constructing the thermal model is to fabricate maps for the region of interest [Adams, 1999]. Interstate 90 through Bozeman Pass will be the area of focus for this thesis. Geographic Information Systems (GIS) experts from Montana State University's Geographic Information and Analysis Center (GIAC) produced the ASCII files for the elevation, road and vegetation maps using ARC/INFO GIS software. The U.S. Geologic Survey provides the digital elevation maps as the source for the elevation file. The terrain file is simply the GIS vegetation ID's from the land cover class and is converted to RadTherm/RT part numbers used to group land covers with similar engineering properties, including emissivity, absorptivity, thermal conductivity, etc.

The elevation and terrain files are loaded into RadTherm/RT to create a new project. However, there is a limitation on the size of a thermal map that can be processed. As the boundaries of the thermal map increase, the number of elements also increases. At a certain point, the calculations for the thermal solution become to complex for computers to solve. Therefore, to optimize the models, a methodology to optimize the number of elements without changing the dimensions of the thermal map was considered beneficial.

One attempt to reduce the size of the thermal map was with the use of a topographic map. The goal was to eliminate the maximum number of elements while keeping all important terrain features that could cause temperature changes on the highway by shade,

radiation exchange, etc. The major concern for this approach is the lack of standards for reducing the boundaries of the map. For example, if a pertinent terrain attribute, such as a mountain peak, is deleted it could greatly influence the temperature output of the terrain or road.

Another method to increase the efficiency of the thermal maps combine the efforts of Montana State University and ThermoAnalytics, Inc. The DEM and vegetation file produced by GIAC for Bozeman Pass is sent to ThermoAnalytics, Inc. to be remeshed. This process includes combining terrain elements to reduce the number of nodes in the map. For instance, four 30-meter square elements are combined to create a single 60x60-meter square element. There are two disadvantages of this process. First, by combining elements, different thermal properties are lost and inaccuracies may be introduced. Second, coarsening the map can be a time-consuming task.

For this project, an analytical approach to optimize the elements used for thermal maps in RadTherm/RT was developed. Chapter 2 gives an overview of heat transfer principles and develops the equations used in the software. View factors are introduced and explained as the basis for eliminating elements for this methodology. A view factor is the fraction of energy that leaves one surface and is absorbed at a second surface. ThermoAnlytics' software determines the radiation relationships between elements that are visible to one another in the model and to the environment [www.thermoanalytics.com]. This algorithm is explored in detail in Chapter 3.

A simple model is introduced in Chapter 3 to describe the energy exchange between elements in different scenarios. The view factors are shown for different orientations and

resulting temperatures are compared. Conclusions from the example demonstrate that energy exchange is highly dependent on angle of slope, distance, and the material surface.

The next section of Chapter 3 describes a detailed methodology used to reduce the number of elements from a thermal map. A four-part C/C++ code was implemented to complete this task. This process is designed to be universal for any region of interest. The goal of this thesis is to significantly reduce the number of elements to improve the efficiency of the map without sacrificing accuracy. This would allow longer stretches of highway to be run with minimal computation time.

CHAPTER 2

BACKGROUND

Heat Transfer

Thermal energy is related to the temperature of matter. The higher the temperature of a material of given mass, the greater its thermal energy. Heat transfer is the exchange of thermal energy through a body or between bodies and occurs when there is a temperature difference. When a temperature gradient exists between two bodies, thermal energy transfers from the one with a higher temperature to the one with a lower temperature.

There are three modes of heat transfer: conduction, convection, and radiation. Any energy exchange between bodies occurs through one of these modes or a combination of them [Incropera and DeWitt, 1996]. The following section gives a brief introduction to each mode.

Conduction

The definition of conduction is the transfer of energy from the more energetic to the less energetic particles of a substance due to interactions between the particles. When there exists a temperature gradient, energy transfer by conduction will occur in the direction of decreasing temperature [Incropera and DeWitt, 1996]. The rate of heat flow due to conduction increases with the thermal conductivity of the material, the cross-sectional area available for it to pass through, and the temperature difference from one

side to the other. As material thickness increases, due to the increased path length, the longer it takes the heat to "flow" from one side to another.

Convection

Convection is heat transfer by mass motion of a fluid such as air or water when the heated fluid is caused to move away from the source of heat, carrying energy with it. Natural convection above a hot surface occurs when hot air expands it becomes less dense, and rises. On the other hand, forced convection is caused by something external such as atmospheric winds or a fan. RadTherm/RT uses the flat plate assumption to calculate the forced convective heat transfer. This is highly dependent on wind speed and temperature difference between the air and surface.

Radiation: Processes and Properties

Radiation is the transfer of energy in the form of electromagnetic waves. This radiation is emitted by objects in all directions without the need of a solid or fluid to transfer the heat [Incropera and DeWitt, 1996]. It uses electromagnetic radiation (photons), which travels at the speed of light and is emitted by any matter with temperature above zero degrees Kelvin (-273 °C). The main types of radiation (from short to long wavelengths) are; gamma rays, X-rays, ultraviolet (UV), visible light, infrared (IR), microwaves, and radio waves. The electromagnetic spectrum classifies radiation according to wavelengths. High-energy physicists and nuclear engineers are primarily concerned with the short wavelength gamma rays, X rays, and UV radiation, while electrical engineers focus on the longer wavelength microwaves and radio waves

[Incropera and DeWitt, 1996]. Thermal radiation is given off by all surfaces that surround us and is in band wavelengths from 0.1 to 100 μm in the electromagnetic spectrum [Sparrow, 1970]. The complete electromagnetic spectrum is illustrated in Figure 1.

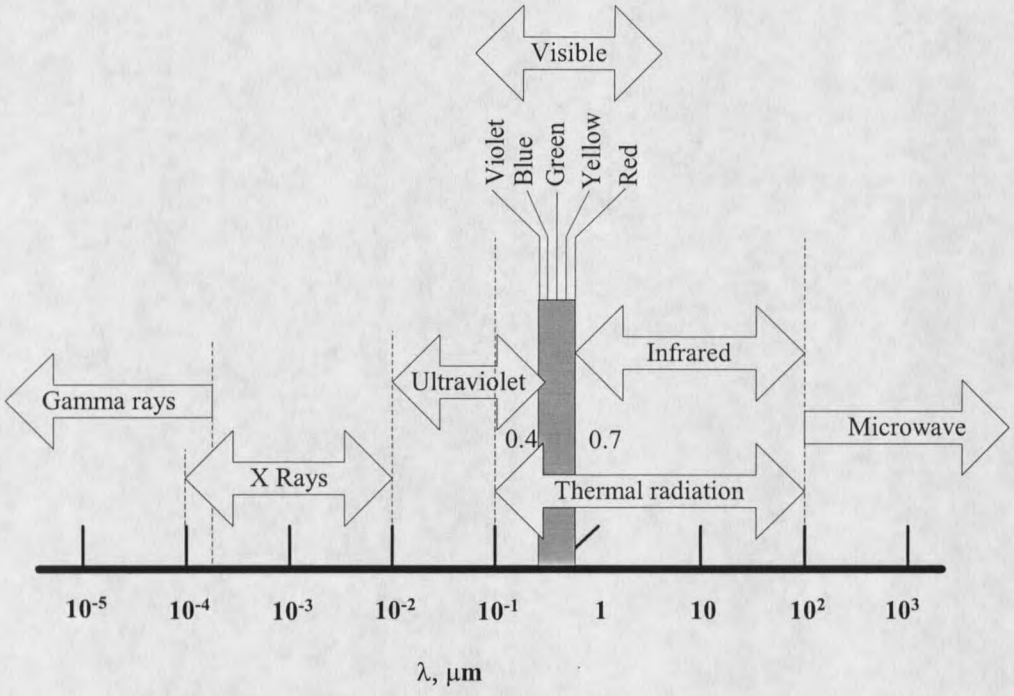

Figure 1. Electromagnetic Spectrum (After Incropera and DeWitt, 1996, Figure 12.3)

Radiation with shorter wavelengths is more energetic. The temperature of the body largely determines the type of radiation emitted. Very hot objects, such as the sun at ~5800 K, emit more energetic radiation including visible and UV. For engineering applications, radiated power is usually in infrared, and sometimes visible or UV. Radiation can be emitted, absorbed, transmitted and reflected by matter (solid, liquid and gas) and can be broken into two parts, shortwave and longwave [Sparrow, 1970].

Shortwave Radiation. The primary source of energy forcing atmospheric motion and many different processes in the atmosphere, at the Earth's surface and in the oceans, is the radiant energy from the sun [Pluss, 1997]. The radiation emitted by the sun is approximately equal to the emission of a blackbody at 5750 K. More than 99% of the energy received from the sun at the top of the earth's atmosphere is in the wavelength range 0.2 to 4.0 μm and known as shortwave radiation [Pluss, 1997]. Shortwave (or Solar) radiation reaches the earth's surface either by being transmitted directly through the atmosphere, direct solar radiation, or by being scattered or reflected to the surface, known as diffuse solar radiation. Diffuse solar radiation is scattered by air molecules, aerosol particles, cloud particles, or other particles.

About 50 percent of shortwave radiation is reflected back into space, while the remaining shortwave radiation at the top of the atmosphere is absorbed by the earth's surface and re-radiated as thermal infrared, or longwave radiation [Pluss, 1997].

Longwave Radiation. Hot objects like the sun emit radiation in shorter wavelengths, while colder bodies, such as the Earth or Earth's atmosphere, emit radiation in longer wavelengths ranging from 4.0 to 100.0 μm. Most longwave radiation reaching the earth surface is emitted from the lowest layers of the atmosphere. The main emitter of incoming longwave radiation is the greenhouse of the earth (e.g. water vapor, carbon dioxide, and ozone) [Pluss, 1997]. Longwave radiation is created from the temperature difference between the atmosphere and the earth's surface. On a clear day the atmosphere is much cooler than the earth's surface and energy is emitted from the surface to the sky.

Radiation Exchange Between Surfaces

All bodies above absolute zero Kelvin temperature radiate energy. Substances emit and absorb radiant energy at a rate depending on the absolute temperature and physical properties of the substance. Not only do they radiate or emit energy, but they also receive and absorb it from other sources [Beckwith, et al, 1993]. Two sets of criteria govern radiative heat transfer between surfaces. The first depends on the material properties, including emissivity, absorptivity, and reflectivity with each depending on temperature.

The second consists of the geometry and the transmission of radiation as a function of direction from the surface and the wavelength of the emitted radiation. This is calculated by the use of view factors. The study of radiation heat transfer in engineering is concerned with the heat loss by emission and heat gain by absorption.

Surface Absorption, Reflection, and Transmission. Incoming shortwave (or solar) radiation that strikes the earth's surface is partially reflected and partially absorbed, in proportion to the surface reflectivity. Figure 2 describes the absorbed, reflected, and transmitted radiation with a semitransparent medium. These incoming portions are divided into fractions of absorptivity (α), reflectivity (ρ), and transmissivity (τ), where

$$\alpha + \rho + \tau = 1. \tag{1}$$

Absorptivity is defined as the fraction of incident radiation (or irradiation) absorbed by an object in relation to a blackbody (range 0-1). Irradiance is the amount of electromagnetic energy incident on a surface per unit time per unit area. This quantity is often referred to as "flux" [Ozisik, 1977].